8276 *Biochemistry* **2010,** *49,* 8276–8289
DOI: 10.1021/bi101280t

BIOCHEMISTRY
including biophysical chemistry & molecular biology
Article

Characterization of the Interaction of β-Amyloid with Transthyretin Monomers and Tetramers[†]

Jiali Du and Regina M. Murphy*

Department of Chemical and Biological Engineering, University of Wisconsin, 1415 Engineering Drive, Madison, Wisconsin 53706

Received August 10, 2010

ABSTRACT: β-Amyloid (Aβ) is the main protein component of the amyloid plaques associated with Alzheimer's disease. Transthyretin (TTR) is a homotetramer that circulates in both blood and cerebrospinal fluid. Wild-type (wt) TTR amyloid deposits are linked to senile systemic amyloidosis, a common disease of aging, while several TTR mutants are linked to familial amyloid polyneuropathy. Several recent studies provide support for the hypothesis that these two amyloidogenic proteins interact, and that this interaction is biologically relevant. For example, upregulation of TTR expression in Tg2576 mice was linked to protection from the toxic effects of Aβ deposition [Stein, T. D., and Johnson, J. A. (2002) *J. Neurosci. 22*, 7380−7388]. We examined the interaction of Aβ with wt TTR as well as two mutants: F87M/L110M, engineered to be a stable monomer, and T119M, a naturally occurring mutant with a tetrameric stability higher than that of the wild type. On the basis of enzyme-linked immunoassays as well as cross-linking experiments, we conclude that Aβ monomers bind more to TTR monomers than to TTR tetramers. The data further suggest that TTR tetramers interact preferably with Aβ aggregates rather than Aβ monomers. Through tandem mass spectrometry analysis of cross-linked TTR−Aβ fragments, we identified the A strand, in the inner β-sheet of TTR, as well as the EF helix, as regions of TTR that are involved with Aβ association. Light scattering and electron microscopy studies demonstrate that the outcome of the TTR−Aβ interaction strongly depends on TTR quaternary structure. While TTR tetramers may modestly enhance aggregation, TTR monomers decidedly arrest Aβ aggregate growth. These data provide important new insights into the nature of TTR−Aβ interactions. Such interactions may regulate TTR-mediated protection against Aβ toxicity.

Alzheimer's disease (AD),[1] the most common age-associated neurodegenerative disease, affects approximately 5 million Americans. Amyloid plaques are one of the primary characteristic features of AD, with β-amyloid (Aβ) as the main protein component of these amyloid plaques. The two common isoforms, Aβ(1−40) and Aβ(1−42), are generated from cleavage of the transmembrane amyloid precursor protein (APP) by β- and γ-secretases (*1*, *2*). Both transgenic animal studies and numerous in vitro studies indicate that Aβ aggregation is causally linked to cellular toxicity, although the exact relationship between Aβ and neuronal toxicity in the progression of AD remains an area of controversy (*3*−*5*). Multiple studies indicate that toxicity arises early and can be attributed to soluble Aβ oligomers and/or protofibrils (*6*, *7*).

Aβ is just one of many amyloidogenic proteins that will, under certain conditions, associate into aggregates with a cross-β structure and fibrillar morphology. Another amyloidogenic protein is transthyretin (TTR): TTR amyloid fibrils are found in patients with familial amyloid polyneuropathy (FAP) or senile systemic amyloidosis (SSA). SSA, characterized by deposition of wild-type TTR, may affect as much as 25% of population over age 80 (*8*). FAP is an inherited disorder, associated with one of numerous TTR mutants (*9*).

TTR is a homotetramer that circulates in both blood and cerebrospinal fluid, with each 14 kDa subunit composed of 127 residues (*10*). Each monomer is a β-pleat sandwich of two four-stranded β-sheets: an inner sheet of strands D, A, G, and H and an outer sheet of strands C, B, E, and F (with one short helix between strands E and F). Monomers assemble into dimers through extensive hydrogen bonding involving strands F and H. The tetramer is formed by hydrophobically driven association of two dimers in a face-to-face manner, held together by loops that project from the edge of the dimer (*10*, *11*). This creates a central channel lined by the inner sheets of the four monomers, where thyroxine (T4) is known to bind (*12*). TTR is also a transporter for retinol binding protein (*13*). In vitro evidence supports a mechanism of amyloid formation whereby TTR tetramers first dissociate into monomers, which then undergo a slight conformational rearrangement and reassemble into fibrils (*14*, *15*). Wild-type (wt) TTR is normally quite stable at neutral pH; dissociation to monomer and subsequent fibril assembly are facilitated at moderately acidic pH. Disease-associated TTR mutants generally have less stable quaternary structures and are more prone to dissociation (*14*, *16*). Hydrogen−deuterium

[†]This work was supported by National Institutes of Health Grant R01 AG033493.

*To whom correspondence should be addressed. Phone: (608) 262-1587. Fax: (608) 262-5434. E-mail: regina@engr.wisc.edu.

[1]Abbreviations: Aβ, β-amyloid; AD, Alzheimer's disease; APP, amyloid precursor protein; BS^3, bis(sulfosuccinimidyl) suberate; CID, collision-induced dissociation; CSF, cerebrospinal fluid; ELISA, enzyme-linked immunoassay; FAP, familial amyloid polyneuropathy; HRP, horseradish peroxidase; LC, liquid chromatography; PBSA, phosphate-buffered saline with azide; SSA, senile systemic amyloidosis; T4, thyroxine; TBST, Tris-buffered saline with Tween; TMB, 3,3′,5,5′-tetramethylbenzidine; TTR, transthyretin.

 Published on Web 08/26/2010

exchange studies along with NMR data indicate that "edge" strands C and D are labile and likely unfold during TTR fibrillogenesis, while strands A, B, E, and G form a stable core that is resistant to unfolding (*17*, *18*). FAP mutants have a less stable core (*19*). TTR fibrils may arise via formation of a non-native interface between strands A and B on different monomers, centered on residues 13 and 31, respectively (*18*).

A growing body of evidence supports the hypothesis that TTR and Aβ interact, and that this interaction is biologically relevant. An early study demonstrated that cerebrospinal fluid (CSF), where TTR is the major protein component, inhibited Aβ amyloid fibril formation (*20*). Several studies have now demonstrated binding between TTR and Aβ, and in some cases, it was also shown that TTR influences Aβ aggregation and reduces Aβ toxicity in vitro (*21*−*25*). Interestingly, some groups have reported that TTR levels in the CSF of AD patients are lower than in healthy controls (*26*−*30*), although other researchers have detected no differences (*31*). Relevant studies have been conducted with Tg2576 transgenic mice, which express the Swedish mutation of APP (APP_{Sw}) and produce extensive Aβ deposits but lack the paired helical filaments and extensive neuronal cell loss one would see in AD (*32*). Stein and Johnson discovered that expression of TTR is greatly upregulated in Tg2576 mice and, importantly, were able to link an increased level of TTR expression to neuroprotection (*33*, *34*). An increased level of TTR expression has been recently confirmed by two other groups (*35*, *36*); interestingly, in one of these studies, decreased TTR levels in aged Tg2576 mice were reported (*35*). Furthermore, Choi et al. (*37*) observed accelerated Aβ deposition in APP_{Sw} mice with heterozygous TTR deletions, and Buxbaum and co-workers (*38*) demonstrated that TTR expression was protective in an APP23 transgenic mouse model. In contrast, Wati et al. (*39*) reported that TTR accelerated vascular Aβ deposits while Doggui et al. (*40*) observed essentially no effect of TTR deletion on plaque deposition in an aggressive mouse AD model. In summary, many, but not all, of the data point to a biologically relevant interaction between TTR and Aβ, thus motivating further investigation into the molecular-level nature of this interaction.

In this study, we aim to further characterize the association between Aβ and TTR. Experiments were conducted with both Aβ(1−40) and Aβ(1−42), and with wt TTR as well as two mutants: T119M and F87M/L110M (M-TTR). T119M is a naturally occurring mutant with a tetrameric stability higher than that of wt (*41*); much of the increased stability appears to be due to subunit contacts rather than tertiary structural changes (*42*, *43*). T119M acts to suppress aggregation when it is incorporated with aggregation-prone mutants into TTR hetero-tetramers (*43*, *44*). M-TTR is a double mutant engineered to be stable as a monomer at neutral pH while fully retaining the native secondary and tertiary structure of wt TTR (*45*).

EXPERIMENTAL PROCEDURES

Expression and Purification of Recombinant TTR. A recombinant plasmid of human transthyretin (pTWIN1-TTR) was constructed as described previously (*46*). The IMPACT-TWIN system was chosen because it allows for expression of protein with a fully human sequence with native N- and C-termini and purification by single-step affinity adsorption without the need for proteases. TTR mutants T119M and F87M/L110M (M-TTR) were prepared with the QuikChange site-directed mutagenesis kit (Stratagene, La Jolla, CA) using pTWIN1-TTR (Met^{-1}) as the template. Plasmids were transformed into ER2566 cells (Stratagene), and cells were grown on LB medium supplemented with 0.1 mg/mL ampicillin. Protein expression was induced with isopropyl β-D-thiogalactopyranoside. Cells were harvested by centrifugation and then lysed [20 mM Tris-HCl, 500 mM NaCl, 1 mM EDTA, 20 μM PMSF, and 1 mM DTT (pH 9.0) containing 8 M urea] as described previously (*46*). Clarified cell lysate was applied to chitin beads (NEB, Beverly, MA) equilibrated with column buffer [20 mM Tris-HCl, 500 mM NaCl, 1 mM EDTA, and 1 mM DTT (pH 9.0)], and protein was cleaved from the column and eluted as described previously (*46*), dialyzed against PBSA [0.01 M Na_2HPO_4/NaH_2PO_4, 0.15 M NaCl, and 0.02% (w/v) NaN_3 (pH 7.4)], and stored at 4 °C. The protein concentration was determined by absorbance at 280 nm, assuming an extinction coefficient of 77600 M^{-1} cm^{-1}.

Characterization of TTR. wt and mutant proteins were analyzed by a linear trap/FT-ICR MS (LTQ FT Ultra) hybrid mass spectrometer (Thermo Fisher Scientific, Bremen, Germany). A single peak was observed for each sample, with molecular masses of 13761.11, 13791.02, and 13763.01 Da for wt TTR, T119M, and M-TTR, respectively, compared to theoretical values of 13761.04, 13791.12, and 13763.08 Da, respectively. SDS gel electrophoresis of boiled samples revealed single bands eluting at 14 kDa; if samples were not boiled, wt TTR and T119M ran as single bands of 55 kDa, indicating formation of tetramers, while M-TTR ran as a 14 kDa (monomer) band. By size exclusion chromatography on a calibrated TSK-GEL G3000SWXL column (TOSOH Bioscience, LLC), M-TTR eluted as a monomer peak while wt and T119M eluted as tetramers. The determination of molecular masses by static light scattering further established that M-TTR was monomeric in solution while wt and T119M were tetramers. An ANS binding assay demonstrated that recombinant wt TTR bound thyroxine, indicating assembly into functional tetramers (*46*). Circular dichroism spectra were obtained to confirm that the secondary structure of the recombinant proteins was virtually identical to that of commercially available TTR purified from plasma. Tryptophan fluorescence emission spectra, with excitation at 290 nm, were recorded; the maximum fluorescence was observed at 338 nm, which is consistent with attainment of the correct tertiary structure.

Sample Preparation. All chemicals were purchased from Fisher (Fair Lawn, NJ) unless otherwise stated. PBSA was double-filtered through 0.22 μm filters (Millex); 8 M urea was prepared in 10 mM glycine-NaOH buffer (pH 10) and then filtered through 0.22 μm filters. Aβ(1−40) (AnaSpec, San Jose, CA) and Aβ(1−42) (American Peptide, Sunnyvale, CA) were used for this study. The Aβ(1−40) stock solution was prepared by directly dissolving lyophilized Aβ(1−40) in 8 M urea to a final concentration of 16 mg/mL (*47*). Although this treatment was sufficient to dissociate preformed Aβ(1−40) aggregates, we found it was not sufficient for Aβ(1−42). Therefore, Aβ(1−42) was pretreated with TFA and HFIP (*48*). Briefly, 0.1 mg of Aβ(1−42) was dissolved in 100 μL of TFA and the mixture sonicated at room temperature for 15 min, and then an additional 1 mL of TFA was added to achieve complete solubilization. The solvent was evaporated under nitrogen, and 1 mL of HFIP was added to redissolve Aβ and then the solvent removed under nitrogen. HFIP treatment was repeated three times to completely remove all residual TFA. The vial was dried overnight under vacuum, leaving a thin film of Aβ on the vial wall. The Aβ(1−42)

stock was prepared by dissolving the film in 8 M urea to a final concentration of 6 mg/mL. Native gel electrophoresis confirmed that Aβ(1−40) and Aβ(1−42) stock solutions were in a monomeric−dimeric state.

ELISA. Mouse monoclonal anti-Aβ antibodies 6E10 and 4G8 (Covance Inc., Emeryville, CA) were selected for this study. These antibodies recognize both monomeric and aggregated Aβ. 6E10 recognizes the N-terminus of Aβ; its epitope is believed to be residues 4−10 (*49*), while 4G8 is reactive to a central sequence, residues 17−24 (*50*, *51*). In preliminary experiments, 6E10 and 4G8 were immobilized on 96-well plates. Detection with the anti-mouse antibody produced uniformly strong color development, as expected; if TTR and the anti-TTR antibody were added to these plates, no nonspecific binding was detected.

ELISA plates (Corning Inc., Corning, NY) were coated with 5 μg/mL wt or mutant TTR (100 μL/well) in coating buffer [10 mM sodium carbonate, 30 mM sodium bicarbonate, and 0.05% NaN_3 (pH 9.6)] overnight at room temperature. For positive controls, 6E10 and 4G8 were coated onto the plate (2.5 and 5 μg/mL, respectively), while for negative controls, only coating buffer was added (blank wells). The plate was washed three times with wash buffer (PBSA with 0.05% Tween 20) and incubated with blocking buffer (5% nonfat dry milk in wash buffer) for 1 h at room temperature. Freshly prepared Aβ(1−40) or Aβ(1−42) was diluted to 5 μg/mL in PBSA and then immediately added to TTR-coated and blank wells (50 μL/well). For background, PBSA was added to TTR-coated wells. The plate was incubated at room temperature or 37 °C for 1 h with gentle shaking. After the plate had been washed, 6E10 or 4G8 was diluted in wash buffer following the manufacturer's instructions added to each well (100 μL/well), and the plate was incubated at room temperature for 1 h. After the samples had been washed, the anti-mouse HRP antibody (Pierce, Rockford, IL) was added to each well and the plate was incubated for 1 h. The plate was washed three times with wash buffer, and then 100 μL of a 3,3′,5,5′-tetramethylbenzidine (TMB) substrate solution (Pierce) was added to each well. After further incubation for 15−30 min, color development was stopped by addition of 100 μL of 2 M sulfuric acid to each well. Absorbance was measured at 450 nm with an EL800 Universal Microplate Reader (Biotek Instruments Inc., Winooski, VT). We reported the Aβ binding intensity as the relative absorbance (A_r) by subtracting the background from sample absorbance.

In some experiments, freshly prepared Aβ(1−40) or Aβ(1−42) was added to TTR-precoated plates and incubated at room temperature for various time intervals [0, 4, 8, and 24 h for Aβ(1−40) or 0 and 24 h for Aβ(1−42)]. Alternatively, aggregated Aβ samples were prepared by 20-fold dilution of an Aβ(1−40) stock into PBSA (to 0.8 mg/mL) followed by overnight incubation at room temperature. Preaggregated Aβ(1−40) was diluted to 5 μg/mL in PBSA right before being added to TTR-precoated wells; plates were processed as described.

Cross-Linking and Analysis by Gel Electrophoresis and Western Blotting. First, 2.5 μL of Aβ(1−40) stock (16 mg/mL in 8 M urea) or Aβ(1−42) stock (6 mg/mL in 8 M urea) was added to 47.5 μL of PBSA (control) or TTR solution (0.1 mg/mL in PBSA) and the mixture incubated at room temperature for 2 h. Then, 50 μL of an Aβ+TTR mixture or TTR alone was mixed with 2 μL of a 25% glutaraldehyde solution and incubated at room temperature for 2 min. The cross-linking reaction was terminated by the addition of 2 μL of 7% (w/v) sodium borohydride in 0.5 M sodium hydroxide. Cross-linked proteins were precipitated with 2 μL of 78% trichloroacetic acid and centrifuged at 14000 rpm for 10 min, and then the supernatant was removed by suction. The precipitate was resuspended in 5% SDS and boiled at 95 °C for 5 min. The samples were analyzed on a Precise 4 to 20% polyacrylamide gradient gel with a 4% stacking gel (Pierce) under constant voltage conditions. In some experiments, Aβ was incubated with TTR overnight before cross-linking and processing as described.

To test whether acid-monomerized TTR would correctly reassemble into tetramers in the presence of Aβ, 34 μL of wt or T119M (0.15 mg/mL, in PBSA) was mixed with 13.5 μL of 100 mM acetic acid (final concentration of 0.1 mg/mL, pH 4.2) and then the mixture incubated at 4 °C for 1 day. For samples with TTR alone, 15 μL of 100 mM NaOH was added to adjust the final pH back to neutral, while for Aβ+TTR samples, 2.5 μL of Aβ(1−40) stock (16 mg/mL in 8 M urea) was added to an acidified TTR solution right before the pH was readjusted with NaOH. TTR or TTR/Aβ solutions were then incubated at room temperature for 2 h before glutaraldehyde cross-linking as described above.

Cross-linked Aβ+TTR samples were separated by SDS−PAGE and then transferred onto a 0.45 μm nitrocellulose membrane (Pierce) at 60 V for 1 h. Membranes were blocked with 5% nonfat dry milk in TBST [20 mmol/L Tris, 150 mmol/L NaCl, and 0.05% (v/v) Tween 20 (pH 7.6)] for 1 h at room temperature or at 4 °C overnight and then reacted with the polyclonal rabbit anti-human TTR antibody (DAKO, Glostrup, Denmark) at a 1:1500 dilution in the same TBST buffer for 1 h at room temperature. The membrane was subsequently treated with anti-rabbit immunoglobulins/HRP (DAKO) at a 1:1500 dilution in TBST at room temperature for 1 h. TTR was visualized by means of an ECL Western Blotting Analysis System (GE Healthcare, Buckinghamshire, U.K.).

Cross-Linking and Tandem Mass Spectrometry Analysis. BS^3 is a homobifunctional *N*-hydroxysuccinimide (NHS) ester with a spacer arm length of 11.4 Å, which reacts with primary amines at pH 7−9. TTR and Aβ were cross-linked with BS^3-d_0/d_4 (Pierce). Briefly, for the M-TTR+Aβ samples, 10 μL of Aβ(1−40) stock (16 mg/mL in 8 M urea, final concentration of 93 μM) was added to 390 μL of an M-TTR solution (0.14 mg/mL or 10 μM, in PBSA). After incubation at room temperature for 2 h, 19 μL aliquots were removed and cross-linking was initiated by addition of 2 μL of a BS^3-d_0/d_4 solution (in a 1:1 mixture of d_0 and d_4 reagent at a concentration of 10 or 20 mM in DMSO), thus yielding 100- and 200-fold molar excesses of cross-linker over M-TTR. The reaction mixture was incubated at room temperature for 30 or 60 min, and then the reaction was terminated by addition of 1 M NH_4CO_3 to a final concentration of 20 mM. Samples were boiled at 95 °C for 5 min followed by separation with SDS−PAGE. Western blotting with the anti-TTR antibody was also performed as described previously. For wt TTR+Aβ samples, 2 μL of Aβ(1−40) stock (16 mg/mL in 8 M urea, final concentration of 93 μM) was added to 78 μL of wt TTR (0.18 mg/mL or 3.3 μM, in PBSA), and the mixture was incubated at room temperature for 2 h. Then, 2 μL of BS^3-d_0/d_4 (in a 1:1 mixture of d_0 and d_4 reagent at 350 mM in DMSO) was added to initiate cross-linking (~2650-fold molar excess of cross-linker over wt TTR). Control samples of cross-linked wt TTR alone were also prepared. The reaction mixtures were incubated at room temperature for 60 min, and then the reaction was terminated with 1 M NH_4CO_3. Samples were boiled at 95 °C for 5 min before being loaded onto the gel.

Cross-linked gel bands of interest were excised, and enzymatic digestion was performed with the *In-gel* tryptic digestion kit (Pierce) following manufacturer's instructions. Reduction and alkylation were conducted to improve the recovery of cystine-containing peptides and minimize the appearance of unknown masses from disulfide bond formation and side chain modification. Trypsin (~100 ng per digestion) in ammonium bicarbonate was used for digestion at 30 °C overnight. Peptide fragments were separated by two-dimensional LC on an Eksigent system (nano2DLC) with two independent binary gradient pumps. The sample was injected into the loading pump, with a water/acetonitrile/ethanol mixture (98:1:1, with 0.1% formic acid) as the solvent, and the flow rate was set at 7 μL/min, with 2 min steps. The peptides were separated with a total run of 55 min using a gradient with the following conditions: 10 to 40% solvent B from 1 to 40 min at a constant flow of 400 nL/min, held at 40% solvent B for 5 min, ramp for 5 min to 90% solvent B, and held for 5 min (solvent A, water with 0.1% formic acid; solvent B, 50:50 acetonitrile/ethanol mixture with 0.1% formic acid). An Agilent Zorbax 300SB C_8 trap column (300 Å pore, 5 μm particle) was used for the first dimension, and the Magic C_{18} column (0.075 mm × 120 mm, 300 Å pore, 5 μm particle) was used for the second dimension.

Nano LC was online coupled with an LTQ mass spectrometer (Thermo Fisher Scientific). The LTQ mass spectrometer was operated in a data-dependent triple-play mode in which each full MS scan (m/z 400−2000, centroid) was followed by zoom scan (5000NL minimum, m/z 10 window, +1 charge rejection) where the centroid ions were automatically selected and fragmented by collision-induced dissociation (CID) using a normalized collision energy of 35% (5000NL minimum, m/z 2.4 isolation, wideband activation). All LTQ spectra were recorded with Xcalibur (version 2.0.5) (Thermo Fisher Scientific). The isotopic pairs were searched and validated manually. Cross-linked peptides were identified using XQuest (http://prottools.ethz.ch/orinner/public/htdocs/xquest/). The mass tolerance (m/z) for precursor ions was 1.0, and the mass tolerance (m/z) for MS/MS was 0.8.

Alternatively, an in-solution-digested sample was prepared. A BS^3-d_0/d_4-cross-linked M-TTR+Aβ sample was prepared as described previously except that the Aβ concentration was 47 μM. After the cross-linking reaction had been terminated, 4−5 volumes of cold acetone (−20 °C) was added, and the sample was kept at −20 °C for at least 2 h followed by centrifugation at 14000 rpm for 10−15 min. After supernatant had been removed, the sample was dried at room temperature before being reconstituted in 100 μL of 8 M urea buffer (8 M urea in 25 mM ammonium bicarbonate). Reducing reagent (5 μL of 200 mM DTT in 25 mM ammonium bicarbonate) was added, and the sample was incubated at 37 °C for 1 h. Alkylation was followed by addition of 20 μL of 200 mM iodoacetamide (IAA) and incubation for 1 h at room temperature in the dark. Reducing reagent (20 μL) was added to consume any leftover IAA. The sample was then diluted to 0.6 M urea with ammonium bicarbonate and digested with trypsin (~1:20 trypsin:protein ratio) at 37 °C overnight. After centrifugation, the supernatant was transferred to a new tube, and ~250 μL of ammonium bicarbonate was added to lower the urea concentration to 0.4 M before GluC was added (~1:20 GluC:protein ratio). Digestion was performed by incubation of the sample at 37 °C overnight.

A model 4800 MALDI TOF/TOF analyzer (Applied Biosystems, Framingham, MA) equipped with a 200 Hz, 355 nm Nd:YAG laser was used for direct peptide profiling of in-solution-digested M-TTR+Aβ sample. Acquisitions were performed in positive ion reflectron mode. Instrument parameters were set using the 4000 Series Explorer software (Applied Biosystems). Mass spectra were obtained by averaging 1000 laser shots covering a mass range m/z of 700−4000. A 6 mg/mL solution of α-cyano-4-hydroxycinnamic acid (CHCA) in 50% (v/v) acetonitrile was used as a matrix. For sample spotting, 0.4 μL of sample was spotted on a MALDI plate and allowed to dry, followed by application of 0.4 μL of matrix solution.

Peptides of the M-TTR+Aβ sample from in-solution double digest were acidified to pH 2 with TFA and analyzed by nano-LC−MS/MS using the Agilent 1100 nanoflow system (Agilent, Palo Alto, CA) connected to a hybrid linear ion trap-orbitrap mass spectrometer (LTQ-Orbitrap, Thermo Fisher Scientific, San Jose, CA) equipped with a nanoelectrospray ion source. HPLC was performed using an in-house-fabricated column with an integrated electrospray emitter made from 360 μm outer diameter × 75 μm inner diameter fused silica tubing. The column was packed with 3 μm C18 particles (Column Engineering, Ontario, CA) to approximately 15 cm. Sample loading and desalting were achieved using a trapping column in line with the autosampler (Zorbax 300SB-C18, 3 μm, 5 mm × 0.3 mm, Agilent). The sample was desalted over 20 min at a flow rate of 15 μL/min using an isocratic HPLC pump to deliver 0.1 M acetic acid and 1% acetonitrile. Peptides were gradient eluted using a binary solvent system with solvent A (0.1 M acetic acid in water) and solvent B [0.1 M acetic acid and 95% acetonitrile (v/v) in water] at 200 nL/min. The gradient elution was achieved with an increase in solvent B content from 1 to 40% over 95 min, from 40 to 60% over 20 min, and from 60 to 100% over 5 min. The LTQ-Orbitrap was set to acquire MS/MS spectra in datum-dependent mode as follows. MS survey scans from m/z 300 to 2000 were collected in centroid mode at a resolving power of 100000. MS/MS spectra were collected on the five most abundant signals in each survey scan requiring that precursors be present in the 2+ or higher charge state, and that they pass the dynamic exclusion criteria. Cross-linked peptides were identified using XQuest (http://prottools.ethz.ch/orinner/public/htdocs/xquest/). The mass tolerance (m/z) for precursor ions was 1.0, and the mass tolerance (m/z) for MS/MS was 0.8.

Light Scattering of Aβ with TTR. The Aβ(1−40) stock was diluted 20-fold (final concentration of 0.8 mg/mL) into filtered PBSA, or PBSA containing 0.1 mg/mL TTR. The samples were rapidly filtered through a 0.45 μm filter directly into a light scattering cuvette placed in a temperature-controlled (25 °C) bath of the index-matching solvent decahydronaphthalene. A Coherent (Santa Clara, CA) argon ion laser at 488 nm was focused on the cuvette, and light scattering data were collected via a Malvern (Southborough, MA) 4700c system, as described in more detail elsewhere (*52*). The average scattering intensity of the sample, $I_s(90°)$, was measured at a 90° scattering angle repeatedly over a 24 h interval. Scattering from toluene, $I_{tol}(90°)$, was measured to account for changes in laser power or aperture, as was background scattering from the solvent, $I_b(90°)$. Data are normalized to the total mass concentration of protein, c_{tot}:

$$I_{norm} = \frac{I_s(90°) - I_b(90°)}{c_{tot} I_{tol}(90°)} \quad (1)$$

Transmission Electron Microscopy (*TEM*). Aβ with M-TTR, wt TTR, or T119M was prepared as described for

light scattering analysis, incubated for 2 weeks at room temperature, stained with NanoW negative stain (Nanoprobes.com, Yaphank, NY), and placed on a pioloform coating grid support film (Ted Pella Inc., Redding, CA). Images of fibrils were taken with a Philips CM120 transmission electron microscope (FEI Corp., Eindhoven, The Netherlands). The number of fibrils and their length were counted and measured manually with ImageJ (National Institutes of Health, Bethesda, MD). The fibril length ranged from 100 to 2250 nm. An array of 10 evenly spaced bins (215 nm each) was chosen initially to count the fibril distribution. Because only a few long fibrils were observed, we grouped the larger bins (530−2250 nm) together.

RESULTS

Binding Interactions between Aβ and TTR. We looked for direct evidence of binding between Aβ and TTR using ELISAs. We used recombinant human wt TTR as well as two mutants: M-TTR (F87M/L110M), an engineered mutant that retains native structure but is a stable monomer (*45*), and T119M, a naturally occurring mutant with greater tetramer stability than wt (*43*, *44*). We were interested in determining whether there were differences between binding of Aβ to monomeric versus tetrameric TTR, or differences in binding of freshly prepared versus preaggregated Aβ to TTR. We used two different antibodies to Aβ, with distinct epitopes, to probe for binding of Aβ to TTR, reasoning that differences in binding of the antibody to Aβ−TTR complexes may shed light on the nature and/or site of any binding interaction. 6E10 and 4G8 react with monomers, oligomers, and fibrils of Aβ (*53*, *54*). 6E10 recognizes the hydrophilic N-terminal sequence (residues 1−16) of Aβ; its epitope is reportedly residues 4−10 (*49*), while 4G8 is reactive to Aβ residues 17−24 (*50*).

Freshly prepared Aβ was added to wells precoated with TTR (wt or mutant). After incubation for 1 h, binding of Aβ to immobilized TTR was probed with 6E10 or 4G8 (Figure 1A). With 6E10 as the probe, binding was observed for all three TTRs, but the signal was significantly higher when M-TTR was immobilized than when either wt or T119M was coated on the wells. With 4G8 as the probe, weakly positive binding was observed for all three TTRs. We repeated this experiment with Aβ(1−42) and obtained results that were very similar to those with Aβ(1−40) (Figure 1B): specifically, the strongest signal was obtained for binding of Aβ to M-TTR when probing with 6E10. We repeated the experiment at 37 °C rather than room temperature and obtained virtually identical results (data not shown).

We repeated the experiments, except after Aβ addition the plates were incubated for longer periods of time before the probe antibody was added. With both Aβ(1−40) (Figure 1C) and Aβ(1−42) (not shown), we observed a substantial (3−12-fold) increase in the amount of 6E10 bound over 24 h. Again, the strongest binding was detected when M-TTR was immobilized.

In another experiment, Aβ(1−40) was preaggregated (1 day at room temperature) prior to being added to TTR-coated wells (Figure 1D). In all cases, the signal was substantially stronger with preaggregated Aβ than freshly prepared Aβ. (Quantitative comparison between fresh and aggregated Aβ is not possible because the difference was greater than the dynamic range of the experiment. When Aβ was prepared and processed under otherwise identical conditions, color development was very strong and immediate with preaggregated Aβ while it took several minutes with fresh Aβ.) Aβ binding was detected for wt- and mutant-coated wells, with the strongest signal again observed with

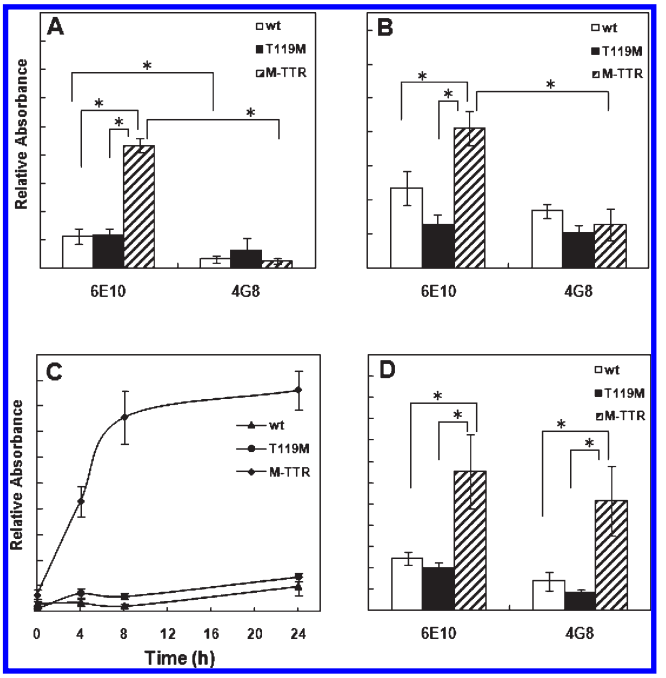

FIGURE 1: ELISA analysis of TTR−Aβ association. wt TTR, T119M, or M-TTR was immobilized on ELISA plates. (A) Freshly prepared Aβ(1−40) was added to each well; after incubation for 1 h and washing to remove unbound material, anti-Aβ antibody 6E10 or 4G8 was used to detect bound Aβ. $*p < 0.05$, and $n = 6$. (B) Freshly prepared Aβ(1−42) was added to each well; after incubation for 1 h and washing to remove unbound material, anti-Aβ antibody 6E10 or 4G8 was used to detect bound Aβ. $*p < 0.05$, and $n = 4$. (C) Binding of Aβ(1−40) to immobilized TTR as a function of time measured with anti-Aβ antibody 6E10. $*p < 0.05$, and $n = 6$. (D) Preaggregated Aβ(1−40) was added to TTR-coated ELISA plates. Anti-Aβ antibody 6E10 or 4G8 was used to detect bound Aβ. $*p < 0.05$, and $n = 6$. When Aβ was added to blank wells (negative controls), no absorbance was detected above empty wells (data not shown); these wells were used as "zero" absorbance.

M-TTR-coated wells. However, in contrast to the case with freshly prepared Aβ, detection of preaggregated Aβ binding with 4G8 and 6E10 was not statistically different.

Cross-Linking of TTR−Aβ Complexes. To further investigate the specific interaction of TTR with Aβ, we cross-linked solutions with glutaraldehyde and then analyzed the resulting complexes by SDS−PAGE and Western blots.

In the first set of experiments, TTR was mixed with freshly prepared Aβ(1−40) (1:8 mass ratio) and incubated at room temperature for 2 h before cross-linking. Samples were boiled and then analyzed by gel electrophoresis (not shown) and by Western blot with anti-TTR antibody detection (Figure 2). Under these conditions, un-cross-linked TTR and Aβ were both monomeric (not shown). On Coomassie-stained gels, crosslinked wt and T119M ran as tetramers while M-TTR ran primarily as a monomer (not shown), demonstrating that the cross-linking conditions preserved the native quaternary structure without inducing excessive aggregation. Cross-linked Aβ exhibited a mix of monomers (~4 kDa) and multimers, with a strong dimer band and what appeared to be weaker trimer, tetramer, and/or pentamer bands. Samples containing Aβ cross-linked with wt TTR or T119M appeared to be a simple additive of TTR and Aβ alone, while with M-TTR/Aβ samples, a series of protein bands with molecular masses in the ~20−30 kDa range were observed. We analyzed these samples further by Western blotting, probing with antibodies to TTR (Figure 2A). No signal was detected with the Aβ

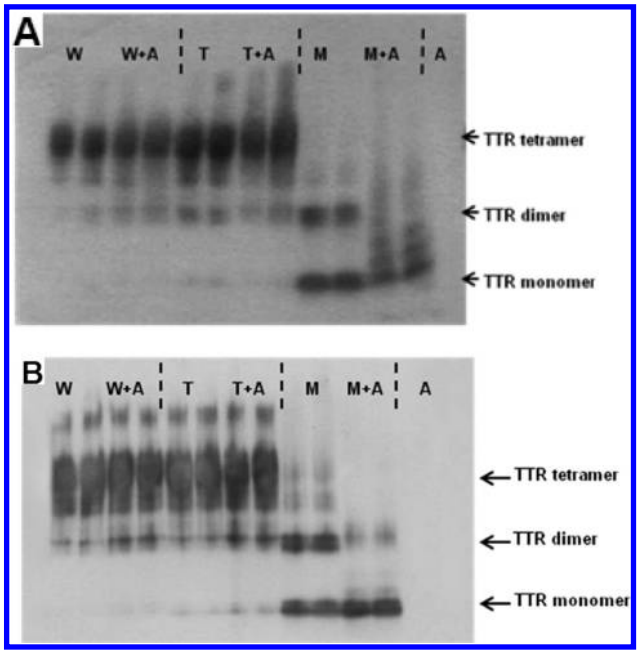

FIGURE 2: Cross-linking of TTR and Aβ. Aβ was incubated with TTR for 2 h and then cross-linked with glutaraldehyde. Samples were boiled and analyzed by SDS−PAGE. Samples were then transferred to a membrane and detected with the anti-TTR antibody. The gels were heavily stained to detect minor species: wt TTR alone (W) or with Aβ (W+A), T119M alone (T) or with Aβ (T+A), M-TTR alone (M) or with Aβ (M+A), and Aβ alone (A). (A) Aβ(1−40) cross-linked with TTR. (B) Aβ(1−42) cross-linked with TTR.

sample, as expected. We observed a small dimer band along with the strong tetramer band for wt and T119M alone. As with the Coomassie-stained gel, for wt and T119M there was no clear difference between TTR alone and TTR with Aβ, while distinct differences were evident upon comparison of M-TTR alone versus M-TTR with Aβ. With M-TTR alone, a dimer band was detected, suggesting that M-TTR formed transient dimers that were locked in place by the cross-linker. Interestingly, when M-TTR was mixed with Aβ, we obtained a ladder of bands. The spacing of the bands suggests that these cross-linked species make up a series of M-TTR−$(A\beta)_n$ complexes. Of additional note is the disappearance of the dimer band from the cross-linked M-TTR−Aβ sample compared to M-TTR alone. These data suggest that Aβ competes with the TTR monomer for self-association. We repeated these experiments with TTR and Aβ(1−42), with similar results (Figure 2B). As with Aβ(1−40), there were no obvious differences between wt or T119M alone and with Aβ, and the dimer band detected was much weaker in the cross-linked M-TTR−Aβ complex than in cross-linked M-TTR.

Next, TTR+Aβ samples were preincubated for 1 day, cross-linked, and then analyzed by SDS−PAGE and Coomassie staining (Figure 3). With M-TTR, we again observed a ladder of complexes upon addition of Aβ. When wt and T119M were incubated for 1 day with Aβ, there was a subtle but measurable and reproducible shift toward higher-molecular mass species, relative to the TTR tetramer band. Furthermore, the TTR−Aβ band was reproducibly "streaky". Such streaks on the gel are frequently considered diagnostic of protein aggregates (*55*). The shift upward in molecular mass and the streaking in the band were observed only with the longer incubation period, suggesting either that Aβ associates only very slowly with TTR tetramers or that Aβ must be allowed to aggregate before it will associate with TTR tetramers.

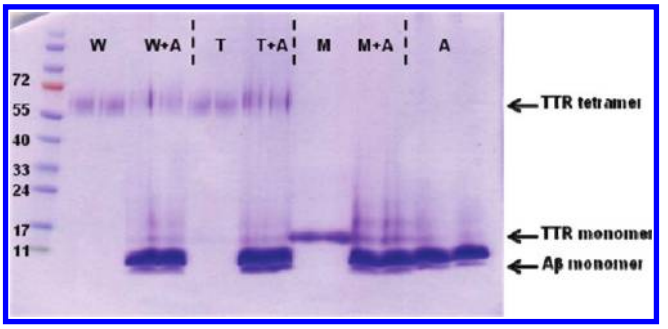

FIGURE 3: Cross-linking of TTR and Aβ. Aβ(1−40) was incubated with TTR for 1 day and then cross-linked with glutaraldehyde. Samples were boiled and then analyzed by SDS−PAGE and detected with Coomassie stain: wt TTR alone (W) or with Aβ (W+A), T119M alone (T) or with Aβ (T+A), M-TTR alone (M) or with Aβ (M+A), and Aβ alone (A).

Reassembly of TTR Tetramers after Acid-Induced Dissociation in the Presence of Aβ. Given the distinctly different interaction of monomeric versus tetrameric TTR with Aβ, we wondered if this was simply a function of the introduced mutations in M-TTR or was related to the loss of quaternary structure. At neutral pH, wt TTR tetramer assembly is strongly favored: the half-life for tetramer dissociation is ~24 h while reassembly occurs within seconds (*56*). wt TTR dissociates slowly to the monomer at moderately acidic pH and will remain monomeric if the sample is held at 4 °C (*14*). Much of the native tertiary structure is retained at acidic pH, although there is evidence of some conformational changes involving the EF helix and adjacent loop (*15*). We obtained monomers from wt TTR by acid dissociation and then tested their reassembly to the tetramer in the absence and presence of Aβ. Specifically, we first dissociated TTR tetramers by incubating a solution at pH 4.2 and 4 °C overnight. Native gels confirmed complete dissociation into monomers under our conditions (data not shown). We then added Aβ and immediately adjusted the pH back to 7.4. Samples were cross-linked after incubation for 2 h. In the absence of Aβ, a return to neutral pH allowed TTR tetramers to reassemble, as assessed by both SDS−PAGE and Western blotting (Figure 4). Overexposure of the Western blot revealed a strong tetramer smear as well as dimer and monomer bands (the latter bands were not visible on the Coomassie-stained gel likely because of their low concentration). There were no apparent differences in the intensity of the tetramer, dimer, and monomer bands between the dissociated and reassembled TTR compared to TTR that had not been acidified at all. This demonstrates that both wt and T119M will fully reassemble into tetramers after acid dissociation followed by a return to neutral pH. With Aβ present during reassembly, most of the TTR again reassembled into tetramers; however, there were faint but distinct bands detectable at ~18 and ~22 kDa. These bands were not present if Aβ was absent; because the bands were detected with the anti-TTR antibody, they contain TTR. The molecular mass of these bands corresponded closely to those obtained when M-TTR was cross-linked with Aβ. These data indicate that complexes between wt TTR monomer and one or two Aβ molecules (TTR_{mon}−Aβ, 18 kDa; TTR_{mon}−$A\beta_2$, 22 kDa) will form if the TTR tetramer is first dissociated. In other words, Aβ binding to TTR monomers competes with reassembly to the tetramer.

Mass Spectrometry Analysis of Cross-Linked TTR−Aβ Fragments. To identify region(s) of TTR that interact with Aβ, we prepared cross-linked samples (wt or M-TTR with Aβ), isolated

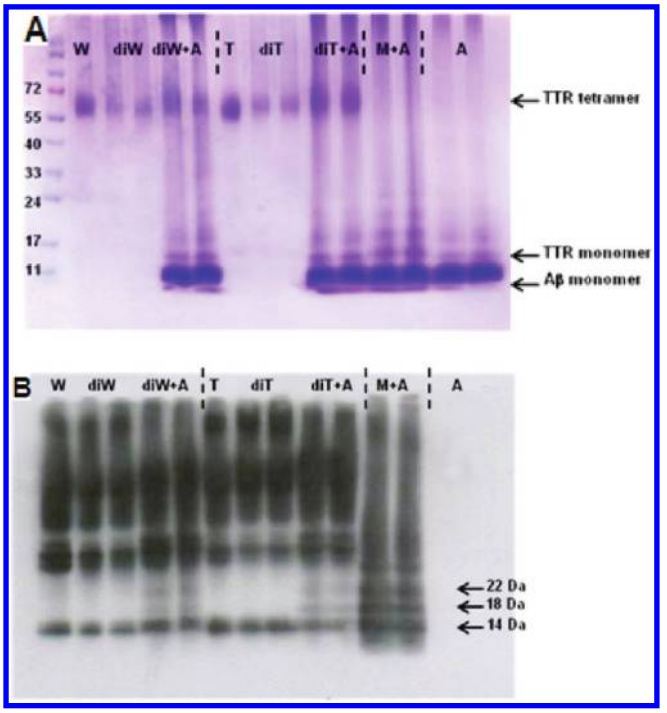

FIGURE 4: Acid dissociation and reassembly of TTR with Aβ. wt TTR was acid-dissociated into monomers and then reassembled at neutral pH in the absence or presence of Aβ(1−40). Samples were cross-linked with glutaraldehyde and then analyzed by SDS−PAGE: wt TTR (W), acid-dissociated and reassembled wt TTR alone (diW) or with Aβ (diW+A), T119M (T), acid-dissociated and reassembled T119M alone (diT) or with Aβ (diT+A), M-TTR with Aβ (M+A), and Aβ alone (A).

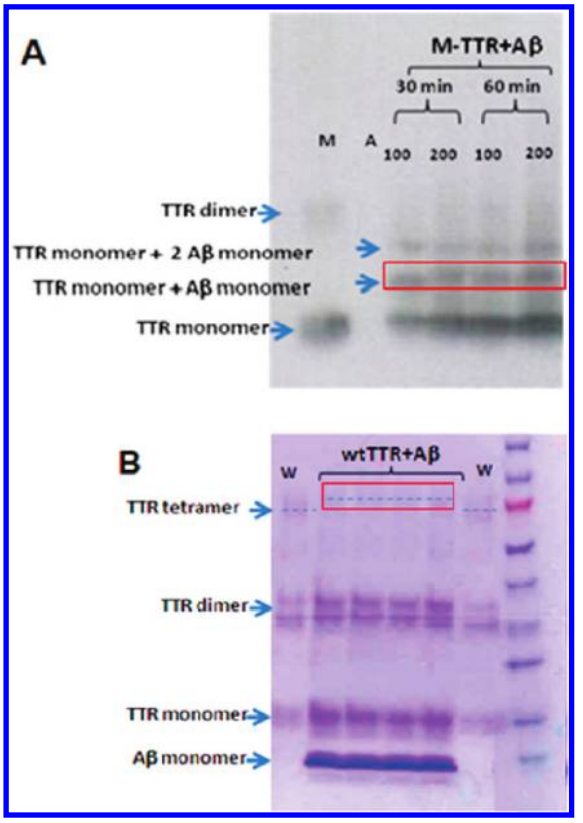

FIGURE 5: Cross-linked samples used in LTQ MS/MS analysis. Aβ-(1−40) was incubated with TTR for 2 h and then cross-linked with BS^3-d_0/d_4. Boxes indicate the gel bands that were excised for enzymatic digestion. (A) M-TTR and Aβ were cross-linked with a 100- or 200-fold molar excess of BS^3-d_0/d_4, and then the reaction was terminated after 30 or 60 min. Samples were analyzed by SDS−PAGE, transferred to a membrane, and detected with the anti-TTR antibody. (B) wt TTR and Aβ were cross-linked with an ~2650-fold molar excess of BS^3-d_0/d_4, and then the reaction was terminated after 60 min. Samples were analyzed by SDS−PAGE. Dashed lines mark the center of protein bands.

the cross-linked material by gel electrophoresis, in-gel-digested the sample, and analyzed fragments by mass spectrometry. The homobifunctional, amine-reactive cross-linker BS^3-d_0/d_4 was used. BS^3 forms amide bond-coupled peptides that cause a characteristic mass shift of 138.067 Da (BS^3-d_0), whereas the partially hydrolyzed cross-linker causes a mass shift of 156.078 Da (BS^3-d_0). BS^3-d_0/d_4 was used to facilitate the identification of cross-linked peptides on the basis of the appearance of isotopic pairs with a 4.025 Da mass difference in the mass spectra.

Figure 5A shows a Western blot of BS^3-d_0/d_4-cross-linked M-TTR and Aβ. At a 100-fold molar excess of cross-linker and with a 30 min reaction time, 1:1 and 1:2 M-TTR−Aβ complexes readily formed. No obvious differences were obtained with further increases in the quantity of cross-linker or the reaction time. The gel bands corresponding to 1:1 complexes were excised and subjected to in-gel tryptic digestion.

For BS^3-d_0/d_4-cross-linked wt TTR and Aβ, a higher molar ratio of cross-linker to TTR (~2650:1) was required to maintain TTR's tetrameric structure when denaturing samples. Even with excess cross-linker, some TTR dimers and monomers were observed (Figure 5B). Further adjusting the quantity of cross-linker or reaction time did not improve the cross-linking efficiency (data not shown). Compared to wt TTR alone, the center of wt TTR−Aβ bands exhibited a slight shift toward a higher mass. Given the fact that the mass of the wt TTR−Aβ complex (1:1) is just 4 kDa higher than that of wt TTR itself, this small mass shift suggests the formation of a cross-linked wt TTR−Aβ complex (1:1). This band was excised and subjected to in-gel tryptic digestion.

The digested peptides were analyzed by LC−MS/MS. On each TTR monomer unit there are eight lysines that can participate in cross-linking (residues 9, 15, 35, 48, 70, 76, 80, and 126). On Aβ there are two lysines (residues 16 and 28). After enzymatic fragmentation of cross-linked materials, intra- and intermolecular cross-linking products as well as "dead-end" peptides (modified by a partially hydrolyzed cross-linker) are obtained. In addition, the mixture contains many non-cross-linked fragments. Because we are interested in finding the interacting sites on TTR and Aβ, the intermolecular cross-linked species are the targeted peptides. To find these, we manually screened for precursor ions with isotopic patterns, indicating the presence of the cross-linker. The corresponding MS/MS data of each isotopic pair were analyzed with XQuest to identify the cross-linking type as well as to unambiguously identify the cross-linking sites. Because reduction and alkylation were performed before enzymatic digestion, the mass increase (57.02 Da) caused by alkylation with iodoacetamide was taken into consideration for each MS/MS calculation.

For the M-TTR−Aβ complex, one (and only one) intermolecular cross-linked product was detected. Intramolecular and dead-end cross-linked peptides were also observed, but not further analyzed. Figure 6A gives the CID spectrum at m/z 1023.29 of the intermolecular cross-linked product ($[M + 4H]^{4+}$). Series of y-type and b-type ions were observed, with the fragmentation patterns identifying the cross-linking site on Lys-9 of M-TTR and Lys-28 of Aβ (Scheme 1A). For the wt TTR−Aβ

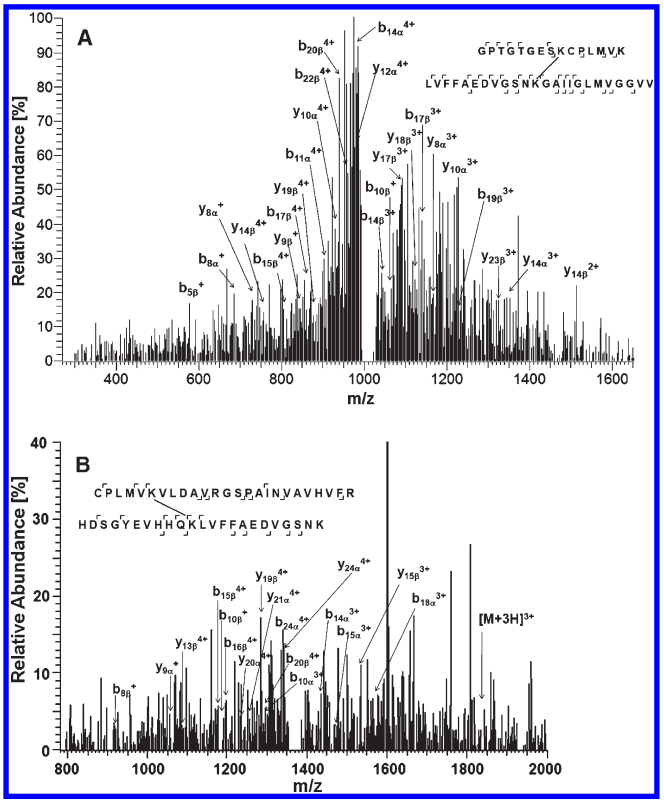

FIGURE 6: MS/MS spectra of cross-linked peptides from trypsin in-gel digestion. (A) CID spectrum of the signal at m/z 1023.29 ($[M + 4H]^{4+}$) corresponding to a cross-linked product between M-TTR (residues 1−15) and Aβ (residues 17−40) cross-linked with a 100-fold excess of BS^3-d_0/d_4, with a reaction time of 30 min. (B) CID spectrum of the signal at m/z 1382.72 ($[M + 4H]^{4+}$) corresponding to a cross-linked product between wt TTR (residues 10−34) and Aβ (residues 6−28) cross-linked with a 2650-fold excess of BS^3-d_0/d_4, with a reaction time of 60 min.

Scheme 1: Fragmentation Patterns (LTQ) of (A) Cross-Linked M-TTR−Aβ Peptides and (B) Cross-Linked wt TTR−Aβ Peptides

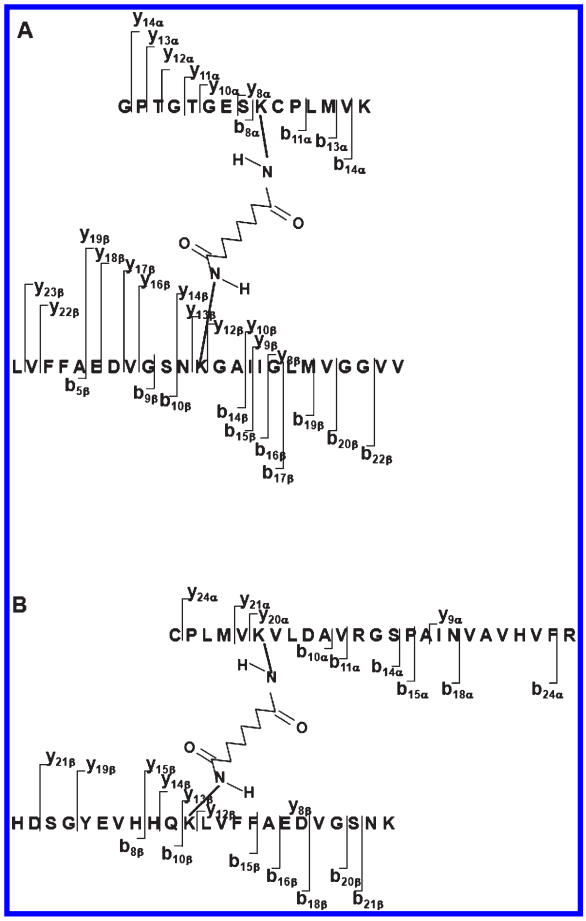

complex, only one intermolecular cross-linked peptide was identified (Figure 6B). MS/MS data analysis indicated that Lys-15 of wt TTR was linked to Lys-16 of Aβ as shown in Scheme 1B. Lys-9 is located near the start of strand A of TTR, while Lys-15 is near the center of strand A. Thus, analysis of both M-TTR and wt TTR clearly implicates residues in strand A of TTR in interactions with Aβ.

The advantage of in-gel digestion is that the cross-linked sample is isolated from non-cross-linked materials, thus reducing the number of fragments present. A possible disadvantage, however, is that some fragments, particularly cross-linked materials, can be difficult to elute from the excised gel band. We decided therefore to conduct in-solution digestion of the cross-linked M-TTR−Aβ complex as an alternative approach, to improve sample recovery. A second enzyme, GluC, was introduced after trypsin to reduce the size of digested fragments. Because of the anticipated additional complexities of the mixture when tetrameric rather than monomeric TTR is used, particularly the large number of intramolecular cross-links, we chose not to attempt this procedure with wt TTR. MALDI and LC/Orbitrap with higher resolution than LTQ were combined as complementary techniques to increase the sequence coverage.

As shown in Figure 7, two intermolecular cross-linked peptides were identified for the M-TTR−Aβ complex. In both cases, Lys-28 was confirmed as the cross-linking site on Aβ (Scheme 2). Figure 7A gives the product ion spectrum at m/z 983.16 ($[M + H]^{4+}$). In this fragment, Lys-15 on TTR is identified as carrying the cross-linker. Thus, consistent with the LTQ studies, strand A of TTR is identified as a region involved in binding to Aβ. Figure 7B shows the CID spectrum of precursor ion at m/z 949.99 ($[M + H]^{4+}$). This fragmentation pattern identifies a cross-linked peptide involving Lys-76 of TTR and Lys-28 of Aβ (Scheme 2). Lys-76 lies near the beginning of the EF helix, the sole helix in TTR.

Effects of TTR on Aβ Aggregation Kinetics and Aβ Aggregate Morphology. We next examined whether the interaction of TTR with Aβ affected Aβ aggregation. The rate of aggregation of Aβ in the presence of each TTR mutant was studied via laser light scattering. The scattering intensity at a 90° scattering angle was measured over time and normalized for the total protein concentration. The scattering intensity is approximately proportional to the average molecular mass of the particles in solution. Experiments were conducted at a low TTR:Aβ ratio (1:8 mass ratio or 1:110 molar ratio), to minimize the contribution of TTR to the total signal. Aβ alone aggregated at a moderate rate over time, as indicated by the increase in intensity. wt TTR had very little effect on the Aβ aggregation rate, while T119M moderately increased the rate of Aβ aggregation over the time course of measurement (Figure 8). The strongest effect was detected with M-TTR, which significantly suppressed Aβ aggregation, lowering both the total intensity and the rate of increase over ~20 h.

Aβ+TTR samples were incubated at room temperature for 2 weeks and then examined by TEM (Figure 9). With Aβ alone, a few long, rigid fibrils were observed while the majority of the

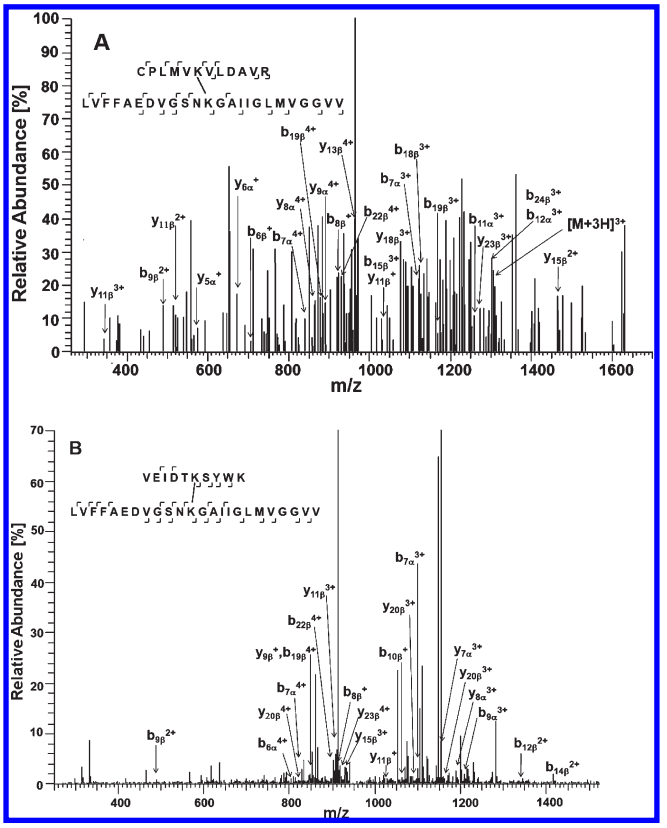

FIGURE 7: MS/MS spectra of cross-linked peptides from trypsin/GluC in-solution digestion. (A) CID spectrum of the signal at m/z 983.16 ($[M + 4H]^{4+}$) corresponding to a cross-linked product between M-TTR (residues 10−21) and Aβ (residues 17−40). (B) CID spectrum of the signal at m/z 949.99 ($[M + 4H]^{4+}$) corresponding to a cross-linked product between M-TTR (residues 71−80) and Aβ (residues 17−40).

aggregates were shorter and semiflexible, with lengths typically around ~100−350 nm. EM images of Aβ alone or with wt TTR were very similar to each other (Figure 9A,B). With the T119M+Aβ mixture (Figure 9C), there appeared to be relatively more long fibrils. The most striking difference was with the M-TTR+Aβ mixture (Figure 9D), where very few long fibrils were observed. We measured the length of 100−200 aggregates for each sample and plotted a histogram of the results to obtain quantitative estimates of the fibril length distribution (Figure 10). This quantitative data confirmed the qualitative observations made from the images. Approximately 15−20% of the Aβ, Aβ+wt TTR, and Aβ+T119M aggregates were long (530−2250 nm), with a slight increase in the fraction of these longest aggregates in the following order: Aβ < Aβ+wt TTR < Aβ+T119M. However, virtually none of the Aβ+M-TTR aggregates fell into this category. At the other end of the size spectrum, only a few percent of the aggregates of Aβ and the Aβ+wt TTR and Aβ+T119M aggregates were shorter than 100 nm, while roughly 50% of the Aβ+M-TTR aggregates were this short. More than 95% of the Aβ+M-TTR aggregates were shorter than 315 nm. Thus, these TEM results are consistent with our light scattering observations, specifically, that T119M modestly enhanced Aβ aggregation while M-TTR strongly suppressed aggregation.

DISCUSSION

Our ELISA data demonstrate that Aβ binds to a greater extent to monomeric (M-TTR) than to tetrameric TTR. Interestingly, detection of binding of freshly prepared Aβ to M-TTR was much stronger with 6E10 than with 4G8. 6E10 binds to the N-terminus

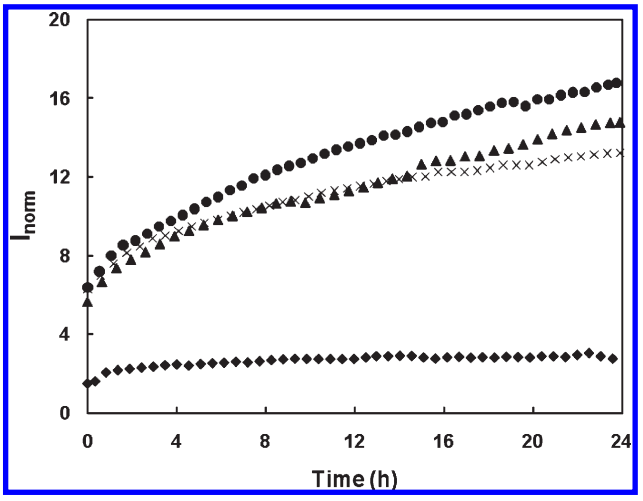

FIGURE 8: Normalized scattering intensity (I_{norm}) at a 90° angle for Aβ alone (×) or Aβ with 0.1 mg/mL wt TTR (▲), T119M (●), or M-TTR (◆). Scattering due to the solvent was subtracted, and results were normalized to the scattering intensity of toluene, to account for changes in laser strength and aperture, and to the mass concentration of the peptide or protein.

Scheme 2: Fragmentation Patterns of Cross-Linked M-TTR−Aβ Peptides (Orbitrap) in Which Aβ Residues 17−40 Were Cross-Linked to (A) M-TTR Residues 10−21 and (B) M-TTR Residues 71−80

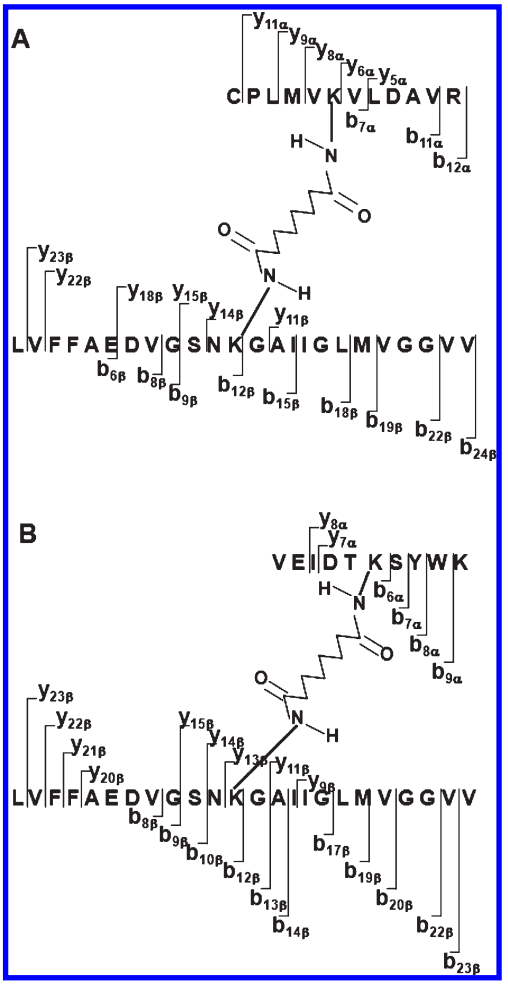

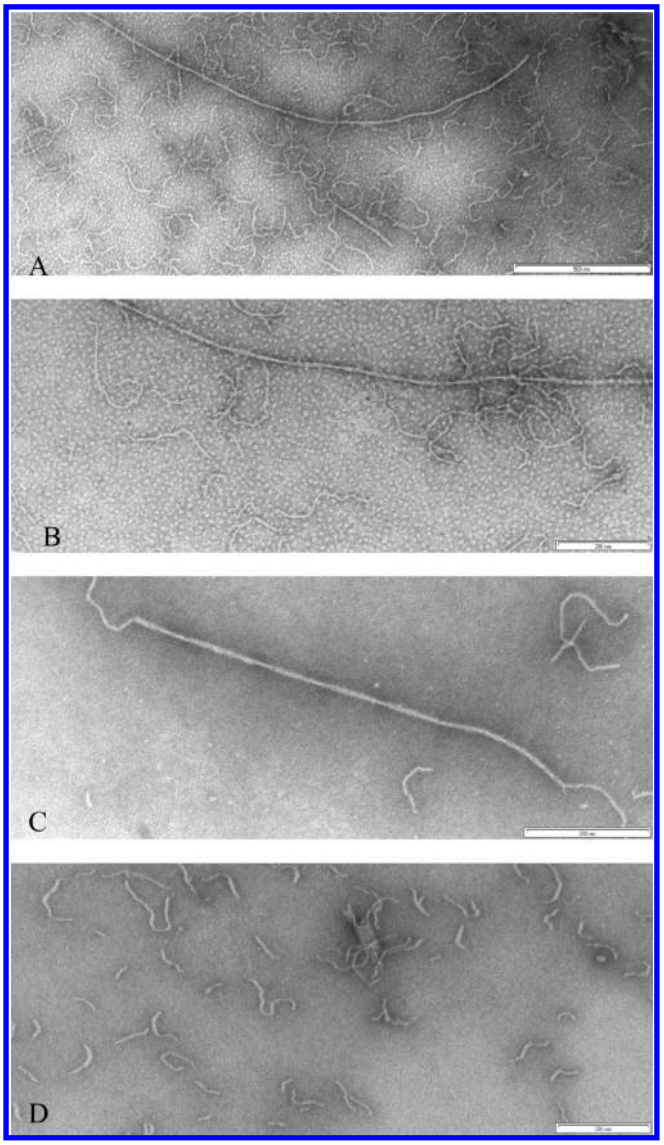

FIGURE 9: TEM images of (A) Aβ alone or Aβ with (B) wt TTR, (C) T119M, or (D) M-TTR. Samples were prepared with 0.8 mg/mL Aβ and 0.1 mg/mL TTR in PBSA. Images were recorded 2 weeks after sample preparation.

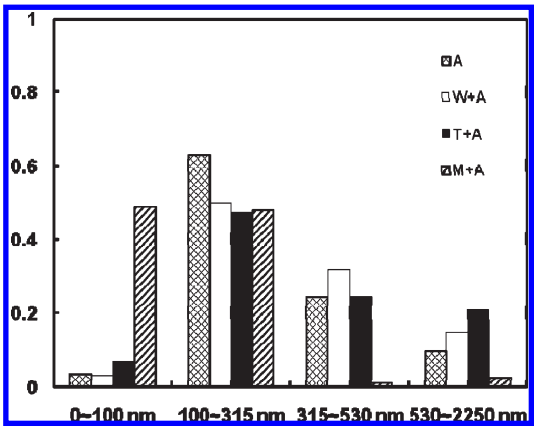

FIGURE 10: Histogram of the Aβ fibril distribution of Aβ alone (A) and Aβ with wt TTR (W+A), T119M (T+A), or M-TTR (M+A).

of Aβ, while the 4G8 epitope lies within residues 17−24. Assuming that 6E10 and 4G8 bind equally to monomeric unbound Aβ, this result suggests that the central domain of Aβ (4G8 epitope) but not the N-terminus (6E10 epitope) is partially blocked by binding to M-TTR. Thus, it is likely that residues in or near the central hydrophobic domain (residues 17−24) of Aβ are involved in the initial binding of Aβ to M-TTR.

Further confirmation that freshly prepared Aβ binds more readily to monomeric than to tetrameric TTR is obtained through cross-linking studies, in which TTR−Aβ complexes were more readily detected with M-TTR than with wt or T119M. Cross-linking of M-TTR alone yielded some dimers, likely because of trapping of transient dimers. Interestingly, these dimers disappeared when Aβ was co-incubated with M-TTR. In its place appeared a ladder of bands with molecular masses corresponding to complexes of M-TTR with one or more Aβ molecules. We checked to see if similar behavior could be detected with wt TTR monomers. Acid-dissociated wt monomers rapidly reassembled into tetramers when the pH was shifted back to neutral. However, if Aβ was present during reassembly, we found that a small fraction of the TTR monomers associated with Aβ, forming a TTR−Aβ_n ladder that was virtually identical to that made with M-TTR and Aβ. Thus, we conclude that it is not the mutations in M-TTR per se that are required for binding of Aβ to TTR monomers; rather, it is the exposure of residues in dissociated TTR that would be sterically blocked or otherwise less accessible in the assembled tetramer. Furthermore, our data demonstrate that Aβ competes, albeit inefficiently, with TTR monomers for assembly into multimers.

Preaggregated Aβ bound to a greater extent to M-TTR than freshly prepared Aβ, but there was no difference between 4G8 and 6E10 detection. Because other researchers have demonstrated that both epitopes are exposed in Aβ aggregates (*54*), we suspect that the 4G8 but not the 6E10 epitope is involved with initial binding of Aβ to M-TTR, that initially bound Aβ provides a template upon which more Aβ is slowly deposited (*57*), that there are multiple Aβ molecules bound per TTR, and that the deposited Aβ aggregates have exposed 4G8 and 6E10 epitopes. In other words, the 4G8:6E10 ratio could be a marker for the relative amount of aggregated versus monomeric Aβ: as this ratio approaches 1:1, the fraction of Aβ bound that is aggregated increases. Our data do not allow us to distinguish formation of aggregates in solution from subsequent deposition and deposition of monomers onto a growing aggregate; most likely, both mechanisms are in play.

From the ELISA results, we found that fresh Aβ bound poorly to tetrameric TTR (either wt or T119M), while binding of preaggregated Aβ was stronger. The difference in binding of preaggregated Aβ to TTR tetramers versus M-TTR, although still significant, was smaller than the difference with fresh Aβ. In almost all cases [Aβ(1−40), Aβ(1−42), freshly prepared, preaggregated], there was no statistically significant difference in 6E10 vis-à-vis 4G8 detection of Aβ bound to TTR tetramers, in contrast to the different 6E10 versus 4G8 pattern with M-TTR. There are several possible explanations. First, there may be no special orientation of Aβ binding to tetrameric TTR, unlike the case with M-TTR: both 6E10 and 4G8 epitopes could be partially blocked. Second, perhaps a different part of Aβ, distant from both epitopes, is involved with binding of Aβ to TTR tetramers, and there is simply less total Aβ bound to tetrameric than to monomeric TTR. Third, there could be binding of Aβ aggregates but not Aβ monomers to tetrameric TTR; this idea is consistent with the notion that the 4G8:6E10 ratio correlates with the degree of aggregation of the bound Aβ.

Consistent with the ELISA results, in cross-linking studies in which Aβ was incubated with wt or T119M, no Aβ−TTR complex was observed when the incubation time was short. However, when samples were incubated for a full day, we noticed a small shift toward higher molecular masses in the tetramer band as well as streaking (Figure 3), usually taken as an indicator of protein aggregates. We did not observe the low-molecular mass ladder that was seen with M-TTR (Figure 2) or with acid-dissociated TTR (Figure 4); in other words, there was no evidence that Aβ strips monomers from stable TTR tetramers. Taken together with the ELISA data, these data suggest that Aβ binds only slowly and relatively weakly to the TTR tetramer, and that the binding is mediated primarily through Aβ aggregates rather than through Aβ monomers.

Costas et al. (*25*) reported no differences in binding of TTR to Aβ monomers, oligomers, or fibrils, in apparent contrast to our findings that Aβ aggregates bind more than monomers. In their experiments, Aβ was prepared at different stages of aggregation and then coated onto wells at pH 9.6, and binding of TTR (at neutral pH) was measured using a competitive inhibition assay. There are several differences between their study and ours that may explain this apparent discrepancy. First, we immobilized a constant quantity of TTR and measured the difference in the quantity of preaggregated versus fresh Aβ bound to TTR, whereas Costas et al. immobilized a constant quantity of Aβ and measured the binding affinity of TTR by varying its concentration. There is also the possibility that the high pH required to coat Aβ in the study by Costas et al. leads to dissociation of preformed aggregates (*58*). Another possibility is that there are differences in TTR stability arising from different preparation methods: this group previously reported that a significant fraction of recombinant wt TTR dissociated into monomers at 0.3 μM (*59*), whereas we observed no dissociation of tetramers under similar conditions (not shown). Alternatively, the discrepancies between their work and ours could be due to other differences in methodology or materials.

We used cross-linking combined with tandem mass spectrometry in an attempt to identify the region(s) on TTR involved with Aβ association. Because our focus was finding heterogeneous intermolecular TTR−Aβ cross-links, we tried to select conditions that would yield TTR−Aβ complexes at a 1:1 ratio and maximize the number of these heterogeneous cross-links compared to homogeneous cross-links (e.g., between TTR monomers or between Aβ monomers). The mixed isotope cross-linker was chosen to facilitate identification of cross-linked peptides in the presence of a large number of other fragments. Gel electrophoresis and excision of the appropriate band were used to isolate the 1:1 TTR−Aβ complex prior to in-gel digestion. Both wt and M-TTR were used in this experiment. Because larger fragments sometimes fail to elute after in-gel digestion, we also used in-solution digestion on a cross-linked mixture of M-TTR and Aβ as a complementary approach.

Using these methods, we identified four cross-linked peptides containing fragments from Aβ and TTR (Schemes 1 and 2). MS/MS analysis localized the cross-linker on TTR to Lys-9 (M-TTR, in-gel digestion), Lys-15 (wt, in-gel digestion), Lys-15 (M-TTR, in-solution digestion), and Lys-76 (M-TTR, in-solution digestion). The positions of these lysines are highlighted (Figure 11). No other sites were detected.

These data clearly identify strand A as a major site of binding between Aβ and TTR, because both Lys-15 and Lys-9 are on or next to this strand. A Kyte−Doolittle analysis identifies this region as a sequence with high hydrophobicity. Strand A is on the inner β-sheet of TTR, lining the channel in the center of the assembled tetramer (Figure 11B). This inner sheet is solvent-exposed in M-TTR, but access would be sterically restricted in the TTR tetramer. This finding could explain why we observed stronger binding of Aβ to M-TTR than to wt. It also explains why Aβ binding to acid-dissociated TTR monomers could compete with reassembly into tetramers.

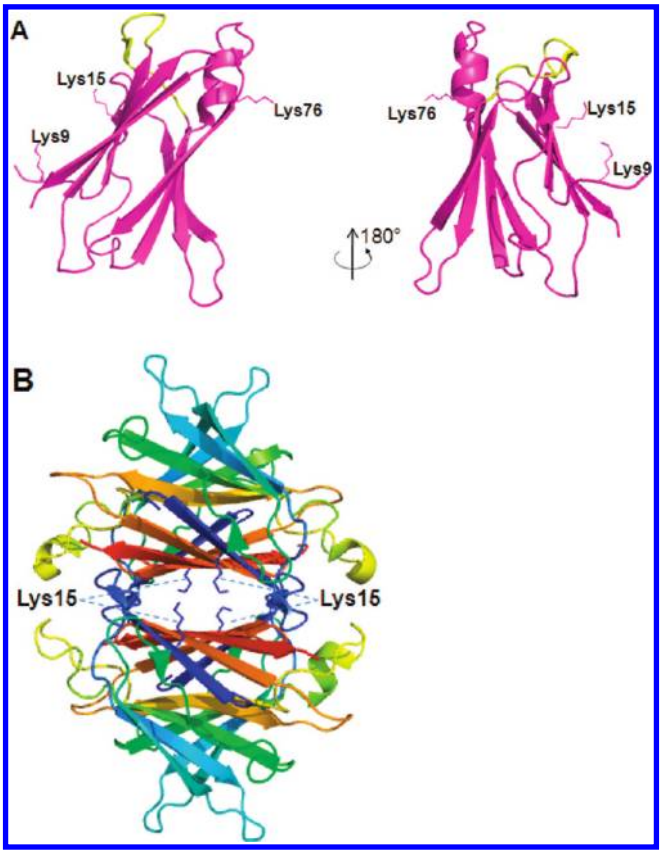

FIGURE 11: (A) Crystal structure of the TTR monomer (Protein Data Bank entry 1DVQ) with the side chains of Lys-9, Lys-15, and Lys-76 indicated that were found to be cross-linked with the Aβ peptide. The AB loop is highlighted in yellow. Because the 10 N-terminal residues were not in the crystal structure because they are disordered, we added this strand by hand to indicate its relative position. (B) Crystal structure of the TTR tetramer in which the side chain of Lys-15 of each monomer is shown.

Strands A, B, E, and G form a highly stable protein core that is resistant to unfolding, while strands C and D are "edge" strands that are fairly labile (*17*, *18*). NMR structural analysis of TTR fibrils supports the hypothesis that strands C and D become more exposed during fibrillogenesis and that a novel interface forms between A strands of different monomers, centered on residue 13, as monomers assemble into fibrils (*18*). Given this, it is tempting to speculate that strand A of TTR is an "amyloidogenic" domain that is recognized by a similar amyloidogenic domain on Aβ.

The involvement of the EF helix in TTR−Aβ association is suggested by the MS/MS data in Figure 7B. In the tetramer, this region protrudes out from the protein surface (Figure 11B). In contrast to strand A, the EF helix is highly solvent exposed and relatively labile. Under acidic conditions (conditions that support tetramer dissociation and subsequent fibrillogenesis), the EF helix and adjacent loop begin to unfold, becoming completely disordered as the pH decreases (*15*). On the basis of strictly steric considerations, one can easily imagine that Aβ binding to or near

the EF helices of the TTR tetramer would be much less restricted than binding to strand A. Furthermore, one can speculate that there may be opportunities for multivalent attachment of Aβ aggregates to two helices along one "side" of the tetramer.

We next examined the effect of TTR on Aβ aggregation, with a focus on the relative size of aggregates. Our light scattering and electron microscopy studies show conclusively that M-TTR arrests Aβ aggregate growth, even at substoichiometric ratios. The long fibrils that appear in samples containing only Aβ disappeared in the presence of M-TTR. In contrast, wt TTR and T119M did not prevent the appearance of fibrillar aggregates and did not arrest Aβ growth; rather, they may have enhanced aggregation slightly.

Previously, we have shown that TTR may accelerate or inhibit Aβ aggregation, depending on the source (purified from plasma vs recombinant) and the degree and nature of modification at Cys-10 (*24*, *46*). Post-translational modification of Cys-10 in plasma and cerebrospinal fluid is common (*60*, *61*). In this study, we were careful to prevent Cys-10 modification, confirmed by mass spectrometry, to reduce this source of variability. We are currently conducting a systematic investigation of the effect of specific Cys-10 modifications on TTR−Aβ association.

On the basis of these combined findings, we propose the following scenario. Briefly, we hypothesize that TTR monomers bind to Aβ, with the interaction involving the residues on or near strand A on TTR, and the central hydrophobic domain on Aβ (near residues 17−24, the 4G8 epitope). This central domain is well-known to be a critical structural element in fibrillar Aβ aggregates (*62*−*64*), and both Lys-16 and Lys-28 of Aβ flank this domain. If a small Aβ aggregate, with an exposed hydrophobic domain, encounters a TTR monomer rather than another Aβ monomer, then binding between the Aβ hydrophobic domain and strand A of the TTR monomer would effectively arrest further growth of Aβ aggregates. This outcome is indeed what we observed by light scattering and EM (Figures 8 and 9).

MS/MS data indicate that TTR tetramers can also bind to Aβ via residues on or near strand A. However, ELISA and cross-linking studies support the conclusion that Aβ does not bind as much to TTR tetramers as it does to TTR monomers. Because strand A lies in the inner sheet of the TTR tetramer, steric constraints would likely limit the extent to which Aβ could be accommodated inside the channel. Data from the experiment in which TTR tetramers were acid-dissociated and then reassembled (Figure 4) suggest that Aβ can compete with TTR monomers for binding during tetramer reassembly, although not particularly effectively. This is reasonable as the rate of TTR tetramer reassembly is extremely fast (*56*).

We tentatively identified the EF helix as another site on TTR that may be involved with TTR−Aβ association. This helix is solvent-exposed in both monomer and tetramer, and one can imagine that binding of both Aβ monomers and aggregates could be easily accommodated. The driving force for association is unknown. The helix is relatively labile, and Lys-76 forms a weak salt bridge with Glu-89 that is lost at low pH (*15*). A highly speculative possibility is that this weak intramolecular salt bridge is replaced with an intermolecular salt bridge between Lys-76 (and possibly Lys-80) on TTR and acidic residues on Aβ, of which there are several in the unstructured N-terminus of Aβ (e.g., Asp-1 and Glu-3). Structural models of Aβ fibrils indicate that the N-terminus remains disordered and is not incorporated into the fibril (*65*). Thus, it is plausible that association between TTR tetramers and Aβ aggregates mediated through the EF helix would not interfere with continued growth of Aβ aggregates, consistent with light scattering and EM data. Also, the limited effect of TTR tetramers compared to monomers on Aβ aggregation could be simply due to less binding. One caveat to this analysis is that we have not yet obtained quantitative data for the relative importance of each site on TTR (strand A and the EF helix) in mediating TTR−Aβ association.

The biological significance of our results remains to be established. There are several intriguing studies suggesting that TTR plays a neuroprotective role by binding to Aβ and that the loss of such protection is linked to the onset of Alzheimer's disease (*33*, *34*, *38*). If true, then characterization of the molecular basis for TTR−Aβ association is needed to elucidate the mechanism of neuroprotection and to understand why such protection might be lost.

ACKNOWLEDGMENT

We thank Matt Tobelmann and Jie Hou for their work in designing, producing, and characterizing the transthyretin mutants, Randall Massey for assistance with TEM, Matt Lawrence, Amy Harms, and Greg Wilt for assistance with mass spectrometry, and Jeff Johnson and Lingjun Li for helpful discussions. MS data were collected at the Human Proteomics Program Mass Spectrometry Facility and at the Biotechnology Program Mass Spectrometry Facility, both at the University of Wisconsin.

REFERENCES

1. Tabaton, M., and Tamagno, E. (2007) The molecular link between β- and γ-secretase activity on the amyloid β precursor protein. *Cell. Mol. Life Sci. 64*, 2211–2218.
2. Gralle, M., and Ferreira, S. T. (2007) Structure and functions of the human amyloid precursor protein: The whole is more than the sum of its parts. *Prog. Neurobiol. 82*, 11–32.
3. Hardy, J. (2002) Testing times for the "amyloid cascade hypothesis". *Neurobiol. Aging 23*, 1073–1074.
4. Wirths, O., Multhaup, G., and Bayer, T. A. (2004) A modified β-amyloid hypothesis: Intraneuronal accumulation of the β-amyloid peptide—the first step of a fatal cascade. *J. Neurochem. 91*, 513–520.
5. Lee, H. G., Casadesus, G., Zhu, X. W., Takeda, A., Perry, G., and Smith, M. A. (2004) Challenging the amyloid cascade hypothesis: Senile plaques and amyloid-β as protective adaptations to Alzheimer disease. *Ann. N.Y. Acad. Sci. 1019*, 1–4.
6. Ferreira, S. T., Vieira, M. N. N., and De Felice, F. G. (2007) Soluble protein oligomers as emerging toxins in Alzheimer's and other amyloid diseases. *IUBMB Life 59*, 332–345.
7. Haass, C., and Selkoe, D. J. (2007) Soluble protein oligomers in neurodegeneration: Lessons from the Alzheimer's amyloid β-peptide. *Nat. Rev. Mol. Cell Biol. 8*, 101–112.
8. Westermark, P., Sletten, K., Johansson, B., and Cornwell, G. G. (1990) Fibril in Senile Systemic Amyloidosis Is Derived from Normal Transthyretin. *Proc. Natl. Acad. Sci. U.S.A. 87*, 2843–2845.
9. Ando, Y., Nakamura, M., and Araki, S. (2005) Transthyretin-related familial amyloidotic polyneuropathy. *Arch. Neurol. 62*, 1057–1062.
10. Hamilton, J. A., and Benson, M. D. (2001) Review. Transthyretin: A review from a structural perspective. *Cell. Mol. Life Sci. 58*, 1491–1521.
11. Wojtczak, A. (1997) Crystal structure of rat transthyretin at 2.5 Å resolution: First report on a unique tetrameric structure. *Acta Biochim. Pol. 44*, 505–517.
12. Chanoine, J. P., Alex, S., Fang, S. L., Stone, S., Leonard, J. L., Korhle, J., and Braverman, L. E. (1992) Role of transthyretin in the transport of thyroxine from the blood to the choroid plexus, the cerebrospinal fluid, and the brain. *Endocrinology 130*, 933–938.
13. Power, D. M., Elias, N. P., Richardson, S. J., Mendes, J., Soares, C. M., and Santos, C. R. A. (2000) Evolution of the thyroid hormone-binding protein, transthyretin. *Gen. Comp. Endrocrinol. 119*, 241–255.
14. Lashuel, H. A., Lai, Z. H., and Kelly, J. W. (1998) Characterization of the transthyretin acid denaturation pathways by analytical ultracentrifugation: Implications for wild-type, V30M, and L55P amyloid fibril formation. *Biochemistry 37*, 17851–17864.

15. Palaninathan, S. K., Mohamedmohaideen, N. N., Snee, W. C., Kelly, J. W., and Sacchettini, J. C. (2008) Structural Insight into pH-induced conformational changes within the native human transthyretin tetramer. *J. Mol. Biol. 382*, 1157–1167.
16. Babbes, A. R. H., Powers, E. T., and Kelly, J. W. (2008) Quantification of the thermodynamically linked quaternary and tertiary structural stabilities of transthyretin and its disease-associated variants: The relationship between stability and amyloidosis. *Biochemistry 47*, 6969–6984.
17. Liu, K., Cho, H. S., Hoyt, D. W., Nguyen, T. N., Olds, P., Kelly, J. W., and Wemmer, D. E. (2000) Deuterium-proton exchange on the native wild-type transthyretin tetramer identifies the stable core of the individual subunits and indicates mobility at the subunit interface. *J. Mol. Biol. 303*, 555–565.
18. Olofsson, A., Ippel, J. H., Wijmenga, S. S., Lundgren, E., and Ohman, A. (2004) Probing solvent accessibility of transthyretin amyloid by solution NMR spectroscopy. *J. Biol. Chem. 279*, 5699–5707.
19. Liu, K., Kelly, J. W., and Wemmer, D. E. (2002) Native state hydrogen exchange study of suppressor and pathogenic variants of transthyretin. *J. Mol. Biol. 320*, 821–832.
20. Schwarzman, A. L., and Goldgaber, D. (1996) Interaction of transthyretin with amyloid β-protein: Binding and inhibition of amyloid formation. *Ciba Found. Symp. 199*, 146–164.
21. Schwarzman, A. L., Gregori, L., Vitek, M. P., Lyubski, S., Strittmatter, W. J., Enghilde, J. J., Bhasin, R., Silverman, J., Weisgraber, K. H., and Coyle, P. K. (1994) Transthyretin sequesters amyloid β protein and prevents amyloid formation. *Proc. Natl. Acad. Sci. U.S.A. 91*, 8368–8372.
22. Tsuzuki, K., Fukatsu, R., Hayashi, Y., Yoshida, T., Sasaki, N., Takamaru, Y., Yamaguchi, H., Tateno, M., Fujii, N., and Takahata, N. (1997) Amyloid β protein and transthyretin, sequestrating protein colocalize in normal human kidney. *Neurosci. Lett. 222*, 163–166.
23. Giunta, S., Valli, M. B., Galeazzi, R., Fattoretti, P., Corder, E. H., and Galeazzi, L. (2005) Transthyretin inhibition of amyloid β aggregation and toxicity. *Clin. Biochem. 38*, 1112–1119.
24. Liu, L., and Murphy, R. M. (2006) Kinetics of inhibition of β-amyloid aggregation by transthyretin. *Biochemistry 45*, 15702–15709.
25. Costa, R., Goncalves, A., Saralva, M. J., and Cardoso, I. (2008) Transthyretin binding to A-β peptide: Impact on A-β fibrillogenesis and toxicity. *FEBS Lett. 582*, 936–942.
26. Riisoen, H. (1988) Reduced prealbumin (transthyretin) in CSF of severely demented patients with Alzheimer's disease. *Acta Neurol. Scand. 78*, 455–459.
27. Serot, J.-M., Christmann, D., Dubost, T., and Couturier, M. (1997) Cerebrospinal fluid transthyretin: Aging and late onset Alzheimer's disease. *J. Neurol., Neurosurg. Psychiatry 63*, 506–508.
28. Castaño, E. M., Roher, A. E., Esh, C. L., Kokjohn, T. A., and Beach, T. (2006) Comparative proteomics of cerebrospinal fluid in neuropathologically-confirmed Alzheimer's disease and non-demented elderly subjects. *Neurol. Res. 28*, 155–163.
29. Gloeckner, S. F., Meyne, F., Wagner, F., Heinemann, U., Krasnianski, A., Meissner, B., and Zerr, I. (2008) Quantitative analysis of transthyretin, tau and amyloid-β in patients with dementia. *J. Alzheimer's Dis. 14*, 17–25.
30. Hansson, S. F., Andreasson, U., Wall, M., Skoog, I., Andreasen, N., Wallin, A., Zetterberg, H., and Blennow, K. (2009) Reduced Levels of Amyloid-β-Binding Proteins in Cerebrospinal Fluid from Alzheimer's Disease Patients. *J. Alzheimer's Dis. 16*, 389–397.
31. Schultz, K., Nilsson, K., Nielsen, J. E., Lindquist, S. G., Hjermind, L. E., Andersen, B. B., Wallin, A., Nilsson, C., and Petersen, A. (2010) Transthyretin as a potential CSF biomarker for Alzheimer's disease and dementia with Lewy bodies: Effects of treatment with cholinesterase inhibitors. *Eur. J. Neurol. 17*, 456–460.
32. Rockenstein, E., Crews, L., and Masliah, E. (2007) Transgenic animal models of neurodegenerative diseases and their application to treatment development. *Adv. Drug Delivery Rev. 59*, 1093–1102.
33. Stein, T. D., Anders, N. J., DeCarli, C., Chan, S. L., Mattson, M. P., and Johnson, J. A. (2004) Neutralization of transthyretin reverses the neuroprotective effects of secreted amyloid precursor protein (APP) in APP(Sw) mice resulting in tau phosphorylation and loss of hippocampal neurons: Support for the amyloid hypothesis. *J. Neurosci. 24*, 7707–7717.
34. Stein, T. D., and Johnson, J. A. (2002) Lack of neurodegeneration in transgenic mice overexpressing mutant amyloid precursor protein is associated with increased levels of transthyretin and the activation of cell survival pathways. *J. Neurosci. 22*, 7380–7388.
35. Tsai, K. J., Yang, C. H., Lee, P. C., Wang, W. T., Chiu, M. J., and Shen, C. K. J. (2009) Asymmetric expression patterns of brain transthyretin in normal mice and a transgenic mouse model of Alzheimer's disease. *Neuroscience 159*, 638–646.
36. Wu, Z. L., Ciallella, J. R., Flood, D. G., O'Kane, T. M., Bozyczko-Coyne, D., and Savage, M. J. (2006) Comparative analysis of cortical gene expression in mouse models of Alzheimer's disease. *Neurobiol. Aging 27*, 377–386.
37. Choi, S. H., Leight, S., Lee, V. M.-Y., Li, T., Wong, P. C., Johnson, J. A., Saraiva, M., and Sisodia, S. S. (2007) Accelerated Aβ deposition in APPswe/PS1DE9 mice with hemizygous deletions of TTR (Transthyretin). *J. Neurosci. 27*, 7006–7010.
38. Buxbaum, J. N., Ye, Z., Reixach, N., Friske, L., Levy, C., Das, P., Golde, T., Masliah, E., Roberts, A. R., and Bartfai, T. (2008) Transthyretin protects Alzheimer's mice from behavioral and biochemical effects of Aβ toxicity. *Proc. Natl. Acad. Sci. U.S.A. 105*, 2681–2686.
39. Wati, H., Kawarabayashi, T., Matsubara, E., Kasai, A., Hirasawa, T., Kubota, T., Harigaya, Y., Shoji, M., and Maeda, S. (2009) Transthyretin Accelerates Vascular Aβ Deposition in a Mouse Model of Alzheimer's Disease. *Brain Pathol. 19*, 48–57.
40. Doggui, S., Brouillette, J., Chabot, J. G., Farso, M., and Quirion, R. (2010) Possible involvement of transthyretin in hippocampal β-amyloid burden and learning behaviors in a mouse model of Alzheimer's disease (TgCRND8). *Neurodegener. Dis. 7*, 88–95.
41. Quintas, A., Saraiva, M. J. M., and Brito, R. M. M. (1997) The amyloidogenic potential of transthyretin variants correlates with their tendency to aggregate in solution. *FEBS Lett. 418*, 297–300.
42. Hammarström, P., Jiang, X., Hurshman, A. R., Powers, E. T., and Kelly, J. W. (2002) Sequence-dependent denaturation energetics: A major determinant in amyloid disease diversity. *Proc. Natl. Acad. Sci. U.S.A. 99*, 16427–16432.
43. Palhano, F. L., Leme, L. P., Busnardo, R. G., and Foguel, D. (2009) Trapping the monomer of a non-amyloidogenic variant of transthyretin: Exploring its possible use as a therapeutic strategy against transthyretine amyloidogenic diseases. *J. Biol. Chem. 284*, 1443–1453.
44. Hammarstrom, P., Schneider, F., and Kelly, J. W. (2001) Trans-suppression of misfolding in an amyloid disease. *Science 293*, 2459–2462.
45. Jiang, X., Smith, C. S., Petrassi, H. M., Hammarstrom, P., White, J. T., Sacchettini, J. C., and Kelly, J. W. (2001) An engineered transthyretin monomer that is nonamyloidogenic, unless it is partially denatured. *Biochemistry 40*, 11442–11452.
46. Liu, L., Hou, J., Du, J., Chumanov, R. S., Xu, Q., Ge, Y., Johnson, J. A., and Murphy, R. M. (2009) Differential modification of Cys10 alters transthyretin's effect on β-amyloid aggregation and toxicity. *Protein Eng., Des. Sel. 22*, 479–488.
47. Pallitto, M. M., and Murphy, R. M. (2001) A mathematical model of the kinetics of β-amyloid fibril growth from the denatured state. *Biophys. J. 81*, 1805–1822.
48. Jao, S. C., Ma, K., Talafous, J., Orlando, R., and Zagorski, M. G. (1997) Trifluoroacetic acid pretreatment reproducibly disaggregates the amyloid β-peptide. *Amyloid 4*, 240–252.
49. Perdivara, I., Deterding, L. J., Cozma, C., Tomer, K. B., and Przybylski, M. (2009) Glycosylation profiles of epitope-specific anti-β-amyloid antibodies revealed by liquid chromatography-mass spectrometry. *Glycobiology 19*, 958–970.
50. Kim, K. S., Wen, G. Y., Bancher, C., Chen, C. M. J., Sapienza, V. J., Hong, H., and Wisniewski, H. M. (1990) Detection and quantitation of amyloid β-peptide with 2 monoclonal-antibodies. *Neurosci. Res. Commun. 7*, 113–122.
51. Thakker, D. R., Weatherspoon, M. R., Harrison, J., Keene, T. E., Lane, D. S., Kaemmerer, W. F., Stewart, G. R., and Shafer, L. L. (2009) Intracerebroventricular amyloid-β antibodies reduce cerebral amyloid angiopathy and associated micro-hemorrhages in aged Tg2576 mice. *Proc. Natl. Acad. Sci. U.S.A. 106*, 4501–4506.
52. Lowe, T. L., Strzelec, A., Kiessling, L. L., and Murphy, R. M. (2001) Structure-function relationships for inhibitors of β-amyloid toxicity containing the recognition sequence KLVFF. *Biochemistry 40*, 7882–7889.
53. Ramakrishnan, M., Kandimalla, K. K., Wengenack, T. M., Howell, K. G., and Poduslo, J. F. (2009) Surface plasmon resonance binding kinetics of Alzheimer's disease amyloid β peptide-capturing and plaque-binding monoclonal antibodies. *Biochemistry 48*, 10405–10415.
54. Necula, M., Kayed, R., Milton, S., and Glabe, C. G. (2007) Small molecule inhibitors of aggregation indicate that amyloid β oligomerization and fibrillization pathways are independent and distinct. *J. Biol. Chem. 282*, 10311–10324.

55. Gallagher, S. R. (2001) One-dimensional SDS gel electrophoresis of proteins. Current Protocols in Protein Science, Chapter 10, Unit 10.11, Wiley, New York.
56. Wiseman, R. L., Green, N. S., and Kelly, J. W. (2005) Kinetic stabilization of an oligomeric protein under physiological conditions demonstrated by a lack of subunit exchange: Implications for transthyretin amyloidosis. *Biochemistry 44*, 9265–9274.
57. Esler, W. P., Stimson, E. R., Jennings, J. M., Vinters, H. V., Ghilardi, J. R., Lee, J. P., Mantyh, P. W., and Maggio, J. E. (2000) Alzheimer's disease amyloid propagation by a template-dependent dock-lock mechanism. *Biochemistry 39*, 6288–6295.
58. Edwin, N. J., Hammer, R. P., McCarley, R. L., and Russo, P. S. (2010) Reversibility of β-amyloid self-assembly: Effects of pH and added salts assessed by fluorescence photobleaching recovery. *Biomacromolecules 11*, 341–347.
59. Quintas, A., Saraiva, M. J. M., and Brito, R. M. M. (1999) The tetrameric protein transthyretin dissociates to a non-native monomer in solution: A novel model for amyloidogenesis. *J. Biol. Chem. 274*, 32943–32949.
60. Biroccio, A., del Boccio, P., Panella, M., Bernardini, S., Di Ilio, C., Gambi, D., Stanzione, P., Sacchetta, P., Bernardi, G., Martorana, A., Federici, G., Stefani, A., and Urbani, A. (2006) Differential post-translational modifications of transthyretin in Alzheimer's disease: A study of the cerebral spinal fluid. *Proteomics 6*, 2305–2313.
61. Lim, A., Prokaeva, T., McComb, M. E., Connors, L. H., Skinner, M., and Costello, C. E. (2003) Identification of S-sulfonation and S-thiolation of a novel transthyretin Phe33Cys variant from a patient diagnosed with familial transthyretin amyloidosis. *Protein Sci. 12*, 1775–1785.
62. Williams, A. D., Portelius, E., Kheterpal, I., Guo, J. T., Cook, K. D., Xu, Y., and Wetzel, R. (2004) Mapping Aβ amyloid fibril secondary structure using scanning proline mutagenesis. *J. Mol. Biol. 335*, 833–842.
63. Kheterpal, I., Chen, M., Cook, K. D., and Wetzel, R. (2006) Structural differences in Aβ amyloid protofibrils and fibrils mapped by hydrogen exchange: Mass spectrometry with on-line proteolytic fragmentation. *J. Mol. Biol. 361*, 785–795.
64. Tjernberg, L. O., Naslund, J., Lindqvist, F., Johansson, J., Karlstrom, A. R., Thyberg, J., Terenius, L., and Nordstedt, C. (1996) Arrest of β-amyloid fibril formation by a pentapeptide ligand. *J. Biol. Chem. 271*, 8545–8548.
65. Paravastu, A. K., Leapman, R. D., Yau, W. M., and Tycko, R. (2008) Molecular structural basis for polymorphism in Alzheimer's β-amyloid fibrils. *Proc. Natl. Acad. Sci. U.S.A. 105*, 18349–18354.